Proceedings of the 39th IAHR World Congress
19–24 June 2022, Granada, Spain
doi://10.3850/IAHR-39WC2521716X20221368

Assessment of Flood Mitigation Capability by Flood Resilience Index

Mrs. Ya-Ting Chang (1), Mr. Yuan-Shun Chang (2), Dr. Hao-Che Howard Ho (3) and Dr. Hong-Yuan Lee (4)

(1,2,3,4) Department of Civil Engineering, National Taiwan University, Taipei City, Taiwan,
haocheho@ntu.edu.tw

Abstract

In recent years, due to the intensification of climate change, the concept of resilience has been widely applied to urban flooding as a basis for disaster management or construction of flooding control. Nevertheless, most studies only define a framework and don't use quantitative index to evaluate resilience. Using the region in New Taipei City, Taiwan as the study area, the 3Di Hydrodynamic Model was used to simulate the time-varied inundation condition under the climate change scenario (700mm in 24 hours). This study established a quantitative Flood Resilience Index (FRI) by selecting physical and socio-economic factors introduced from ISO 14090 climate change risk guideline. The results could assess the degree of resilience of an area over time and assist the government to make efficient decisions under limited resources in the flood.

Keywords: Flood resilience index; Climate change risks; Disaster management; Flood simulation; Design storm pattern

1. INTRODUCTION

Under the influence of global climate change, the frequency of extreme events with intensive rainfall increases the risk of flooding. The highly urbanization, at the same time, could pose a serious threat toward the drainage system and even cause the detriment to the lives and properties of human society (Burian et al., 2002; Miller et al., 2017; UNISDR, CRED, 2015). The new concept for the urban stormwater management is necessary. Therefore, the resilience which combined with vulnerability and recovery ability began to be applied to the strategies of the disaster prevention (R. Berke et al., 2006; Leichenko, 2011; Jordan et al., 2012; Asprone et al., 2013; Kamissoko et al., 2019). Apparently, it is difficult to accurately quantify the resilience of a region. Nevertheless, the current researches on urban resilience have only provided assessment framework, and have not accurately proposed operational or quantitative resilience indicators yet (Bulti et al., 2019; Lyu et al., 2019; Zhong et al., 2020). In the study of resilience assessment framework, Jelena et al. (2013) proposed the concept of the FRI which assesses the ability of one area to withstand the shock by flooding and return to the original social-economic level. Chen et al. (2019) applied the concept of FRI on Munich to define quantifiable indicators of urban flood resilience. The selection of factors to be considered in the assessment of resilience is very comprehensive. In addition to infrastructure and economic losses, which are easier to quantify, institutional and community resilience are increasingly seen as key factors. (L.Cutter et al., 2008; Batica, 2014; Dadson et al., 2017).

The purpose of this study is to construct a resilience index for the flooding mitigation. Resilience is considered to be the combination of the vulnerability and recovery ability. According to the AR5 Synthesis Report for the impacts of climate change (IPCC, 2014) and the ISO14090 adaptation to climate change, the vulnerability can be defined as the destructiveness to a city which has been affected by a disaster, it can also be subdivided into the interaction of sensitivity, hazard and exposure (Few, 2003; TCCIP, 2018; WMO UNISDR, 2012; ISO, 2019). As for the recovery ability is the speed and capacity to return to the equilibrium state after a disaster event. Therefore, the severity of flooding, the population, the level of social-economic and the community participation of disaster prevention work are the main influencing factors. The effect of time should be regarded as an important variable for the aforementioned factors (Kong, 2016). This study proposed the time-varied FRI and included different factors of the densely populated urban area with the extreme rainfall events as a simulation condition, and 3Di Water Management dynamic model was conducted to simulate the flooding severity of the study area. According to the results of stimulation, the FRI assessment was divided into event phase and post-disaster recovery phase. By analyzing the impacts on the index in different scenarios of intensity and design storm pattern, we hope to evaluate the best timing for disaster prevention resources to be invested.

2. STUDY AREA AND MATERIAL

The study area was located in the Zhonghe District and Yonghe District, which has a total area of 25.86 km^2. These two District are in New Taipei City (as shown in Figure 1) that is the most populous special municipality in Taiwan.

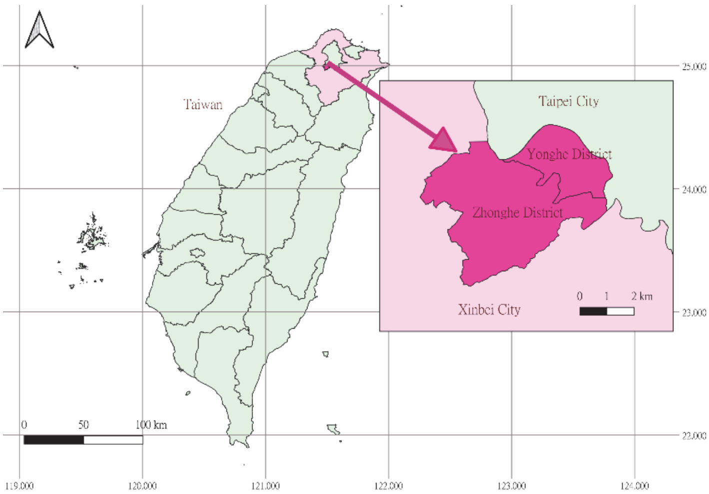

Figure 1. Location of Zhonghe District and Yonghe District

2.1 Social Development

Due to the government's immigration policy in the 1960s and the rapid development of Taipei City, many people moved to live in this area which results in the overpopulation in contrast to the original urban plan. Nowadays, the population of Yonghe District is 215 thousand, and the population density is 38.5 thousand per km^2, surpassing 21.16 thousand per km^2 of Macau. With dense buildings and narrow streets, the development here has reached saturation.

The land use types in the study area include industry, business, residential, green field, hydrology, office/school, and traffic (as shown in Figure 2). Table 1 shows the parameters input in numerical model for different land use. The current use pattern is mainly residential. The traffic part includes asphalt roads, MRT station, impermeable sidewalks and parking lots, the green space includes all parks and woodlands and a few agricultural lands, hydrology contains river and open channels.

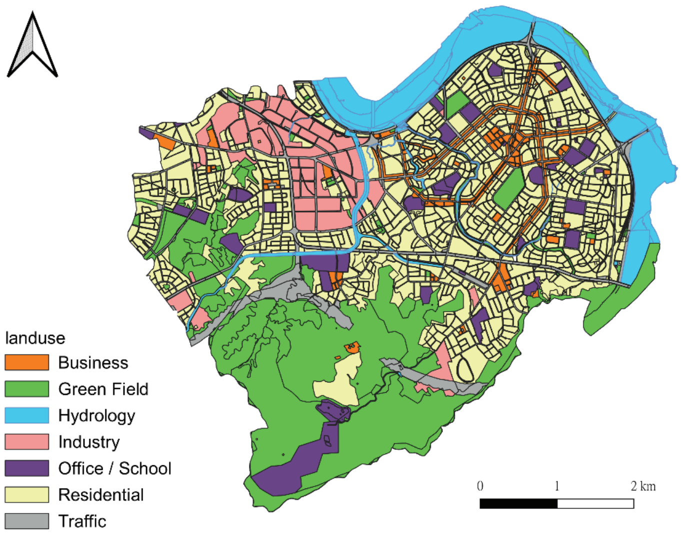

Figure 2. Land use in the study area

Table 1. Parameters for different land use

Land use	Manning n	Infiltration(mm/day)	Interception(m)
Green Field	0.03-0.15	54.66-147.01	0.0014-0.0029
Traffic	0.01	0	0
Hydraulic	0.01	0	0
Residential	0.05	42.76	0.003
Industry	0.05	34.02	0.003
Office/School	0.01-0.05	18.35-64.66	0.0016-0.003
Business	0.05	18.35	0.003

2.2 Geography and Climate

Soil properties here are mostly loamy soil and sandy soil. The southern part of the study area is hilly and terrace, with a maximum elevation of over 300 meters. However, because Xindian River flows through the northern part of the study area, it is an alluvial plain and lots of local low-lying area with elevations down to about three meters, causing flooding during heavy rains.

The study area was a subtropical humid climate zone. According to official records, the average annual precipitation was about 2,173 mm, in contract to 900mm, the average precipitation in the world.

This study included extreme rainfall events under climate change as a simulation scenario to assess the flood resilience of this area. Based on the research from NCDR (National Science and Technology Center for Disaster Reduction), in future period of 2075 to 2099, global climate change scenario with RCP8.5(Representative Concentration Pathways) scenario cause 50-year 24-hr precipitation was 700mm, 100-year 24-hr precipitation was 850mm. Citing these data, this study designed the rainfall distribution as shown in Figure 3.

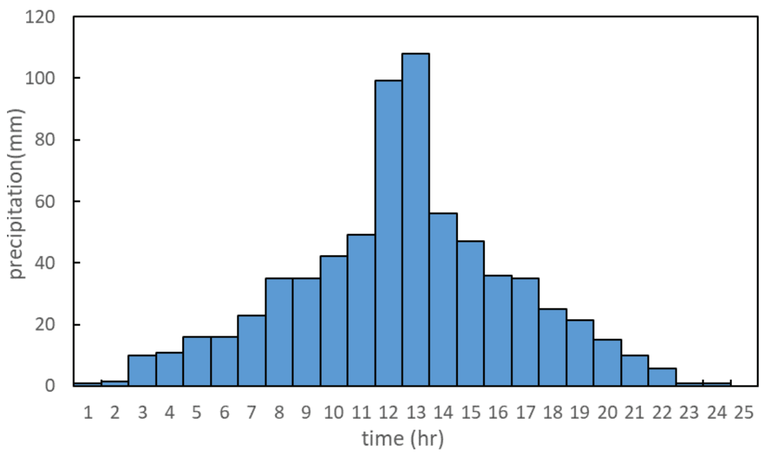

Figure 3. Rainfall distribution for the simulation scenario (700mm in 24 hours)

3. THEORY AND METHODS

3.1 Climate Change Risks

In 2019, ISO (International Organization for Standardization) released ISO 14090, specified principles, guidelines and requirements for adaptation to climate change. In this vein, ISO further drafted 14091, which described how to understand the relationship between risk and vulnerability to the potential impacts of climate change. When the system was exposed to risk, there may be some adaptations to reduce the risk, which could be called vulnerability. Table 2 shows three components of risk defined by ISO 14091. This study would use this framework to design resilience index.

Table 2. three components of risk

	definition	examples of factor
hazard	physical events or trends related to climate or non- climate (ex. their physical effects)	heatwave, typhoon, drainage
exposure	distribution of people or assets in space	population distribution
sensitivity	the degree of adverse or beneficial effects of the hazard	crop yields due to temperature

3.2 Flood Resilience Index: FRI

The study established FRI to evaluate resilience of an urban area during flooding events. Urban resilience could be divided into vulnerability and recovery, which has been widely applied in many articles; nevertheless, they never propose a quantitative and time-dependent index such like Figure 4. When a disaster occurs, FRI would drop from 1 in event phase. While in the recovery phase, the disaster no longer caused additional damage, and FRI would restore to near its original state. The demarcation point between the event phase and the recovery phase that could be the basis for government to relieve in disaster must be calculated by equations in chapter 3.3.

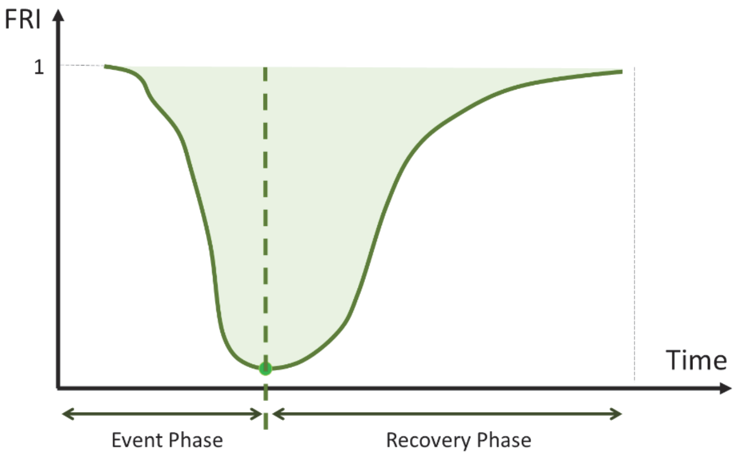

Figure 4. schematic of FRI

3.3 Structure of the FRI

FRI was composed of three main indicators, which were hazard, exposure and sensitivity. They had the same weight for the FRI and each indicator contained corresponding factors.

3.3.1 Hazard Indicator

Hazard indicator was related to the physical phenomenon of flooding. There were three same-weight factors; moreover, each factor would be defined a reference value. If the reference value was exceeded, the factor score would be zero, which the system was in a state of collapse.

- Flooding depth factor: The equation is shown below, as in Eq. [1]. The deeper flooding depth was, the higher possibility it would directly and immediately endangered the safety of life and property. According to the definition given by NCDR, the reference value (H_{ref}) was set at 0.5m; the depth of 0.25m was considered to be the beginning of the flooding event, additionally.

$$F_H(t) = \begin{Bmatrix} 1-(H_i(t)/H_{ref}) & ,if\ \mathrm{H}_{\mathrm{ref}} \geq H_i(t) \\ 0 & ,if\ \mathrm{H}_{\mathrm{ref}} < H_i(t) \end{Bmatrix} \qquad [1]$$

  where, H_i was the average flooding depth in different village.
- Flooding area factor: The equation is shown below, as in Eq. [2]. The larger the flooding area was,

the more difficult resident could maintain the normal life function in their village. The reference value (A_{ref}) was set at 50% of each district area.

$$F_A(t) = \begin{cases} 1-(A_i(t)/A_{ref}) & ,if\ \mathrm{A_{ref}} \geq A_i(t) \\ 0 & ,if\ \mathrm{A_{ref}} < A_i(t) \end{cases} \quad [2]$$

where, A_i was the average percentage of flooding area in different village.

- Flooding duration factor: The equation is shown below, as in Eq. [3]. The longer duration was, the more probability that drainage system might be inoperable giving rise to serious disasters. As long as the water depth was greater than 0.25m, the flooding duration was accumulated and it would be defined as flooding event. However, the recovery ability starts to work and duration becomes to 0 hour when the last 0.25m appeared. The reference value (D_{ref}) was set 8 hours.

$$F_D(t) = \begin{cases} 1-(D_i(\mathrm{t})/D_{ref}) & ,if\ \mathrm{D_{ref}} \geq D_i(t) \\ 0 & ,if\ \mathrm{D_{ref}} < D_i(t) \end{cases} \quad [3]$$

where, D_i was the flooding duration in different village.

Finally, hazard indicator could be calculated as in Eq. [4].

$$I_{hazard}(t) = \frac{1}{3} \times \left\{ F_H(t) + F_A(t) + F_D(t) \right\} \quad [4]$$

3.3.2 Exposure Indicator

In this study, exposure indicator was related to spatial distribution of population and businesses in the study area. The denser the population and businesses were, the damage would be more concentrated. The score of exposure indicator were all 1 except during the flooding event. By collecting all data, we could define the density of first quartile as the reference value (P_{ref}, B_{ref}). In this study, P_{ref} equaled to 356 people/ ha, and B_{ref} equaled to 102 businesses / ha. If the density of the district was less than reference value, the district was viewed as less susceptible to damage than other district s in the event of a disaster. The factor during the flooding event could be calculated as Eq. [5] and Eq. [6].

- Population density factor:

$$F_P = \begin{cases} 1 & ,if\ \mathrm{P_{ref}} \geq P_i \\ P_{ref}/P_i & ,if\ \mathrm{P_{ref}} < P_i \end{cases} \quad [5]$$

where, P_i was the population density in different district.

- Businesses density factor:

$$F_B = \begin{cases} 1 & ,if\ \mathrm{B_{ref}} \geq B_i \\ B_{ref}/B_i & ,if\ \mathrm{B_{ref}} < B_i \end{cases} \quad [6]$$

where, B_i was the businesses density in different district.

Finally, exposure indicator during the flooding event could be calculated as in Eq. [7].

$$I_{\exp osure} = \frac{1}{2} \times \left\{ F_P + F_B \right\} \quad [7]$$

3.3.3 Sensitivity Indicator

In this study, sensitivity indicator was related to community participation and economic level which included salary and turnover. The reference value of salary and turnover, S_{ref} and T_{ref}, would be set in the form of third quartile. The better community participation and economy were, the more prepare before disaster or rehabilitation after disaster they had. The score of sensitivity indicator were all 1 in the beginning, then it would decrease in exponential form during flooding event and rise in exponential form until reaching to 1 while the recovery force started to work. The factor could be calculated as Eq. [8] to Eq. [10].

- Salary factor and Turnover factor:

$$F_E(t): E = \{salary, turnover\},\ F_E(t) = \begin{cases} 1 & ,if\ t < t_f \\ e^{-(1-x)t} & ,if\ t_f \le \mathrm{t} \le t_f + D \\ e^{(1-x)t} & ,if\ t_f + D \le \mathrm{t} \le t_f + 2D \\ 1 & ,if\ t_f + 2D < \mathrm{t} \end{cases} \quad [8]$$

where, D was flooding duration, and

$$x_i : E_i = \{salary(S_i), turnover(T_i)\},\ x_i = \begin{cases} E_i/E_{ref} & ,if\ \mathrm{E_{ref}} \ge E_i \\ 1 & ,if\ \mathrm{E_{ref}} < E_i \end{cases} \quad [9]$$

- Community participation factor:

$$F_V(t) = \begin{cases} 1 & ,if\ t < t_f \\ e^{-(1-x)t} & ,if\ t_f \le \mathrm{t} \le t_f + D \\ e^{(1-x)t} & ,if\ t_f + D \le \mathrm{t} \le t_f + 2D \\ 1 & ,if\ t_f + 2D < \mathrm{t} \end{cases} \quad [10]$$

where, x was a custom score of 0 to 1 based on government certification and the number of disaster prevention education.

Finally, sensitivity indicator could be calculated as in Eq. [11].

$$I_{sensitivity}(t) = \frac{1}{3} \times \{F_S(t) + F_T(t) + F_V(t)\} \quad [11]$$

The whole FRI simply combined with three indicators, as in Eq. [12].

$$FRI(t) = I_{hazard} \times I_{\exp osure} \times I_{sensitivity} \quad [12]$$

4.CONCLUSIONS

After the 3Di simulation (simulation time was 53 hours), the flooding impact with the scenario (700mm per 24 hours) was evaluated in each district of the study area from the maximum inundation depth map, as shown in Figure 5. The pink blocks represent the districts in the study area. The results show that 17 districts would have the significance change in FRI where the average inundation depth was greater than 0.25m for more than 5 hours and no low-lying terrain was there to affect the result. During the flooding event, the flooding depth and area factor exceeded the reference values resulting in a low score for the hazard indicator (as shown in Figure 6). Moreover, it shows that the duration factor dominated the time-varied variables for the most severe period (as shown in Figure 6).

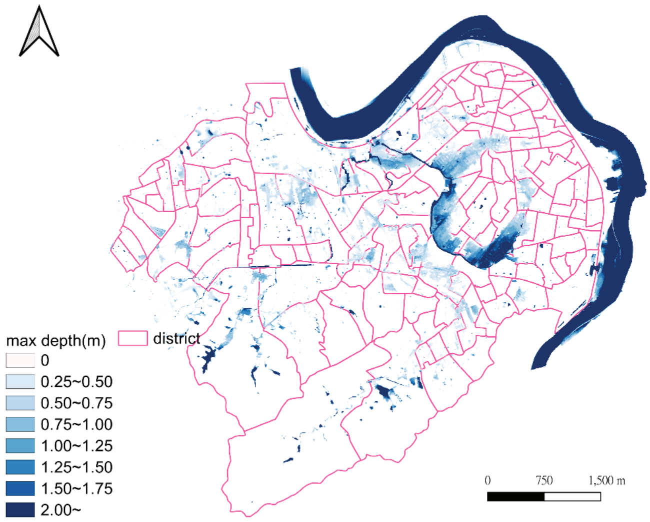

Figure 5. The inundation situation of the study area

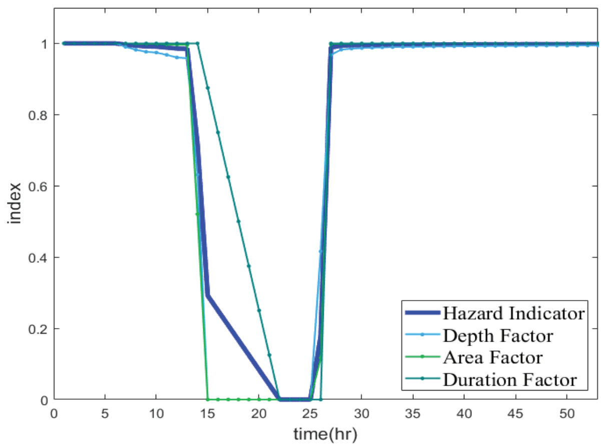

Figure 6. The relationship between the three factors in the hazard indicator (district 46 for example)

In the severe situation, the results demonstrate that the social-economic condition of the district is important. The lower social-economic condition is and the weaker recover ability is. The government should pay priority attention to the exposure and sensitivity indicators of these districts which are low social-economic so that it can prepared in advance and mitigate the flooding impact.

The level of social-economic would play an important role on the resilience index. Figure 7 shows the comparison of districts 31 and 96. They have same duration and similar depth leading to close lowest point of hazard indicator; however, their social-economic condition is different, as shown in table 3. The turnover gap was so large that a rapid decline in the sensitivity indicator of the district 96 contributed to the lowest FRI score 0.0521 comparing to the lowest FRI of the district 31 with 0.156. Furthermore, we could observe the smaller FRI score during the early stage of recovery phase. All phenomena indicate that district 96 had less resilience to flooding and weaker recovery ability than the district 31 due to lower sensitivity indicator. The government should strengthen relief to prevent in district 96 after the 21st hour, and could adjust the resource allocation among all districts depending on the FRI score.

Table 3. The social-economic parameters of district 31 and district 96

	F_P	F_R	**Salary(S)**	**Turnover(T)**
district 31	0.5733	0.6458	1	1
district 96	0.5775	0.8434	0.9110	0.552

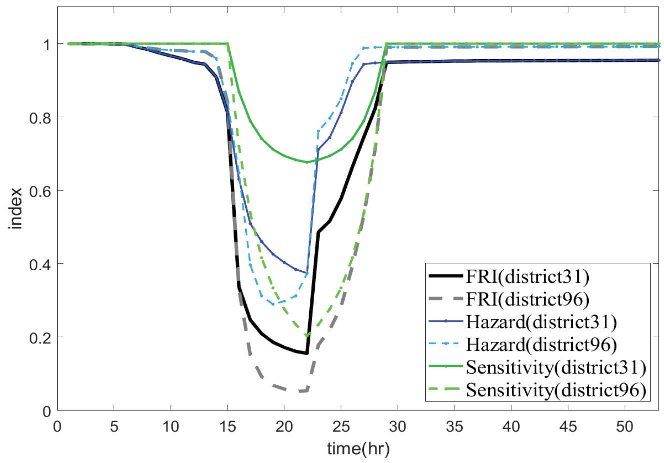

Figure 7. The index of district 31 and district 96 changing with time

In the past, the government might simply consider the inundation depth of flooding for the allocation of rescue. Because of the limited index, it is difficult to decide the priority to be rescued and maximize the resource allocation. The design of the FRI with multi-aspect and time-varied features considers physical flooding conditions, economic conditions, and community conditions that gives the support for decision makers in disaster management for the government.

5. ACKNOWLEDGEMENTS

This research was supported by the grant from Research Center for Sustainable Development and Disaster Mitigation in Urban and Rural Regions, National Taiwan University. We thank colleagues from Research Center for Sustainable Development and Disaster Mitigation in Urban and Rural Regions who provided insight and expertise that greatly assisted the research.

6. REFERENCES

Kuan-Hui Elaine Lin, Hsiang-Chieh Lee, Thung-Hong Lin. (2017). How does resilience matter? An empirical verification of the relationships between resilience and vulnerability. Nat Hazards 88:1229–1250.

Asprone, D., Cavallaro, M., Latora, V., Manfredi, G., and Nicosia, V. (2013). Assessment of urban ecosystem resilience using the efficiency of hybrid social-physical complex networks. *Computer-Aided Civil and Infrastructure Engineering 29*(February).

Burian, S., and Edwards, F. (2002). Historical perspectives of urban drainage. *Proceedings of 9th International Conference on Urban Drainage*, Portland, USA (2002).

Berke, P.R., and Campanella, T.C. (2006). Planning for Postdisaster Resiliency. The ANNALS of the American Academy of Political and Social Science, 604(1), 192-207.

Batica, J. (2013). METHODOLOGY FOR FLOOD RESILIENCE INDEX. *International Conference on Flood Resilience Experiences in Asia and Europe*, Sep. 5-7(2013), Exeter, United Kingdom.

Bulti, D.J., Girma, B., and Megento, T.L. (2019). Community flood resilience assessment frameworks: a review. *SN Applied Sciences,* 1(12), 1663.

Cutter, L.S., Barnes, L., Berry, M., Burton, C., Evans, E., Tate, E., and Webb J. (2008). A place-based model for understanding community resilience to natural disasters. *Global Environmental Change*, 18(4), 598-606.

Chen, K.F., and Leandro, J. (2019). A Conceptual Time-Varying Flood Resilience Index for Urban Areas: Munich City. *Water,* 11(4), 830(April).

Chang YS, Ho HC, Huang LY. (2021). Role of Low Impact Development on Urban Flood Resilience Index. *Advancing Earth and space science Fall Meeting 2021*, Dec. 13-17(2021), New Orleans, USA.

Dadson, S., Hall, J.W., Garrick, D., Sadoff, C., Grey, D., and Whittington, D. (2017). Water security, risk, and economic growth: Insights from a dynamical systems model. *Water Resources Research,* 53(8), 6425-6438.

Few, R. (2003). Flooding, vulnerability and coping strategies: local responses to a global threat. Progress in Development Studies, 3(1), 43-58.

ISO. (2019) 14090:2019 Adaptation to climate change-Principles, requirements and guidelines. Greenhouse gas management and related activities, *International Organization for Standardization*.

Jordan, E., and Javernick-Will, A. (2012). Measuring Community Resilience and Recovery: A Content Analysis of Indicators. Construction Research Congress 2012, May. 21-23(2012), Indiana, USA.
Kong, J. (2016). AN ORIGINAL MODEL OF INFRASTRUCTURE SYSTEM RESILIENCE. *CSCE RESILIENT INFRASTRUCTURE Annual Conference*, Jun. 1-4(2016), London, United Kingdom.
Kamissoko, D., Nastov, B., Benaben, F., Chapurlat, V., Bony-Dandrieux, A., Tixier, J., Amendeep, and A., Daclin, N. (2018). Continuous and multidimensional assessment of resilience based on functionality analysis for interconnected systems. *Structure and Infrastructure Engineering*, 15(4), 427-442.
Leichenko, R.M. (2011). Climate Change and Urban Resilience. Current Opinion in Environmental Sustainability, 3(3), 164-168.
Lyu, H.M., Shen, S.L., Zhou, A., and Yang, J. (2019). Perspectives for flood risk assessment and management for mega-city metro system. *Tunnelling and Underground Space Technology 84*(February), 31-44.
Miller, J., and Hutchins, M. (2017). The impacts of urbanisation and climate change on urban flooding and urban water quality: A review of the evidence concerning the United Kingdom. *Journal of Hydrology: Regional Studies*, 12(C), 345-362.
NCDR. (2019). Study of climate change risk assessment and adaptation application of water resources from IPCC risk definition. *National Science and Technology Center for Disaster Redution*.
UNISDR WMO. (2012). Disaster Risk and Resilience. *On System Task Team on the POST-2015 UN Development Agenda*, May(2012).
Zhong, S., Clark, M., Hou, X.Y., Zang, Y., and Fitzgerald, G. (2013). Development of hospital disaster resilience: Conceptual framework and potential measurement. *Emergency Medicine Journal*, 31(11).